DC-Informative Joint Color-Frequency Modulation for Visible Light Communications

Qian Gao, *Member, IEEE*, Rui Wang, *Member, IEEE*, Zhengyuan Xu, *Senior Member, IEEE*, and Yingbo Hua, *Fellow, IEEE*

***Abstract*—In this paper, we consider the problem of constellation design for a visible light communication (VLC) system using red/green/blue light-emitting diodes (RGB LED), and propose a method termed dc-informative joint color-frequency modulation (DCI-JCFM). This method jointly utilizes available diversity resources including different optical wavelengths, multiple baseband subcarriers, and adaptive dc-bias. Constellation is designed in a high-dimensional space, where the compact sphere packing advantage over lower dimensional counterparts is utilized. Taking into account multiple practical illumination constraints, a non-convex optimization problem is formulated, seeking the least error rate with a fixed spectral efficiency. The proposed scheme is compared with a decoupled scheme, where constellation is designed separately for each LED. Notable gains for DCI-JCFM are observed through simulations, where balanced, unbalanced, and very unbalanced color illuminations are considered.**

***Index Terms*—Color-frequency modulation, constellation design, DC-informative, intensity modulation/direct detection (IM/DD), visible light communication (VLC).**

I. Introduction

TO satisfy the increasingly higher data rate demands, visible light communication (VLC) has drawn tremendous interest from both industry and academia as a promising complement to traditional radio frequency communication (RFC) that suffers from spectrum saturation [1]–[3]. The maturing of light-emitting diodes (LED) manufacturing techniques during the recent decade largely boosts the trend of replacing traditional lighting systems with LED alternatives for both indoor and outdoor illumination purposes, and the resulting infrastructures are ready for deployment of VLC. It is a low-cost technology, where one can use the simple intensity modulation and direct detection (IM/DD) techniques. In addition, one can enjoy a bunch of additional advantages such as eye-safety, high security and causing no electromagnetic inference.

Manuscript received August 5, 2014; revised February 5, 2015; accepted February 24, 2015. Date of publication March 3, 2015; date of current version March 19, 2015. This work was supported in parts by the National Basic Research Program of China under Grant 2013CB329201, National Natural Science Foundation of China under Grant 61171066, and Shenzhen Peacock Plan (No. 108170036003286).

Q. Gao and Z. Xu are with the Key Laboratory of Wireless-Optical Communications, Chinese Academy of Sciences, School of Information Science and Technology, University of Science and Technology of China, Hefei 230026, China (e-mail: qgao@ustc.edu.cn; xuzy@ustc.edu.cn).

R. Wang is with the Tongji University, Shanghai 200092, China (e-mail: liouxingrui@gmail.com).

Y. Hua is with the University of California, Riverside, CA 92521 USA (e-mail: yhua@ee.ucr.edu).

Color versions of one or more of the figures in this paper are available online at http://ieeexplore.ieee.org.

Digital Object Identifier 10.1109/JLT.2015.2408620

VLC is both unique from and similar to RFC. With regard to the uniqueness of VLC, it only allows positive and real signals to drive the LEDs as intensities (a non-informative dc-bias is typically used); its channel especially for indoor environment is much more slower varying than an RFC counterpart; baseband waveforms modulate the LEDs directly instead of being up-converted first, etc. As for the similarity between VLC and RFC, many existing RFC techniques can be applied, although possibly with non-straightforward modifications to VLC systems, e.g., optical multiple input multiple output (O-MIMO) [4], optical orthogonal frequency division multiplexing (O-OFDM) [5]–[7], and other advanced signal processing techniques [8]–[16]. These (and relevant) works take advantage of various diversities a VLC system provides, such as spatial diversity, frequency diversity, color diversity, and adaptive dc-bias [10]–[12], to improve system performance. However, to the best of our knowledge, there is lack of research on joint leverage of these diversities for a more efficient VLC constellation design under illumination constraints.

In this paper, the joint exploration of multiple diversities is achieved through constellation design in high-dimensional space. This space is formed by several degrees of freedoms including adaptive dc-bias, baseband subcarriers and multiple wavelengths corresponding to red/green/blue (R/G/B) LED lights. According to the fundamental idea that spheres can pack constellation points more compactly in a higher dimensional space, a constellation with larger minimum Euclidean distance (MED) can be expected in a higher dimensional space.[1] This MED maximization problem is formulated in a non-convex optimization form, and is then, relaxed to a convex optimization problem by a linear approximation method. Key practical lighting requirements are taken into account as constraints, e.g., the optical power constraint, average color constraint, non-negative intensity constraint, luminous efficacy rate (LER) requirements, and color rendering index (CRI) when white-light illumination is required [17]–[19].

For RFC, one well-known shortcoming with utilizing multiple subcarriers is the excessive peak-to-average power ratio (PAPR) problem introduced, which can cause severe nonlinear distortion to degrade system performance. Plenty of methods have been proposed to reduce PAPR (see [20] and references therein). In fact, when using multiple subcarriers for VLC, high PAPR is also a very severe issue, due to the limited linear dynamic range of amplifiers and LEDs. This paper shows that such distortion can be avoided by formulating the dynamic range

[1] For a communication system, the system symbol error rate (SER) is governed by the MED with working SNRs [11].

requirement as (convex) constraints of the optimization problem. In such way, distortion control becomes an offline process or a by-product of constellation design.

The remainder of this paper is organized as follows. In Section II, we first provide an overview of dc-informative modulation schemes for optical communications. DC-informative multicarrier modulation is introduced as a power efficient alternative to traditional non-dc-informative optical OFDM configurations.

In Section III, we propose a constellation design method termed DCI-JCFM leveraging multiple diversities jointly, under lighting constraints such as color of illumination, luminous efficacy rate, non-negative intensity, signal dynamic range, and flickering-free. Color rendering index is also considered if a system is "balanced," while is disregarded if a system is "unbalanced" or "very unbalanced" depending on the required illumination color.

In Section IV, we discuss the pros and cons of using dynamic range constraint, short time PAPR constraint and long time PAPR constraint. In Section V, we provide simulation results to verify the significant performance gains of the proposed method over a decoupled method for balance, unbalance, and very unbalanced systems. Finally, Section VI provides conclusions.

II. Overview of DC-informative Modulation for Optical Communications

Optical communications based on IM/DD has a unique feature of requiring all signals modulating the LEDs to be positive (and real), so multiple schemes are proposed accordingly such as the well-known asymmetrically clipped optical OFDM (ACO-OFDM), dc-biased optical OFDM (DCO-OFDM) and optical multisubcarrier modulation (MSM). These schemes all discard the dc-bias at the receiver, which causes significant power loss. The dc-informative modulation schemes were then proposed such that 100% optical power is used for data transmission (see [10], for single carrier case, and [11], for multiple carrier selective fading case). To be specific, consider the channel model

$$y_i(t) = \alpha\eta s_i(t) * h(t) + v(t) \qquad i \in [1, N_c] \tag{1}$$

where $s_i(t)$ is a symbol waveform mapped from $\mathbf{b}_i$ that contains N_b bits of information, $*$ denotes the convolution operator, $h(t)$ is either flat-fading or selective-fading channel, $v(t)$ denotes white noise, $y_i(t)$ is the received signal, η and α are electrical-to-optical and optical-to-electrical conversion factors respectively,[2] and $N_c = 2^{N_b}$ stands for the constellation size.

Unlike the conventional optical MSM, where a non-informative (typically constant) dc-bias is imposed on all symbols [8], our system design method adopts informative dc-bias, which varies from symbol to symbol, and the basis function for dc-bias is

$$\phi_1(t) = \sqrt{\frac{1}{T_s}}\Pi\left(\frac{t}{T_s}\right) \tag{2}$$

where $\Pi(t)$ is a rectangular waveform defined as

$$\Pi(t) = \begin{cases} 1, & \text{if} 0 \le t < 1 \\ 0, & \text{otherwise.} \end{cases} \tag{3}$$

[2]We assume $\alpha\eta = 1$ without loss of generality.

and the bases for in-phase and quadrature subcarriers are

$$\phi_{2k}(t) = \sqrt{\frac{2}{T_s}}\cos(2\pi f_k t)\Pi\left(\frac{t}{T_s}\right) k = 1, 2, \ldots, K \tag{4}$$

$$\phi_{2k+1}(t) = \sqrt{\frac{2}{T_s}}\sin(2\pi f_k t)\Pi\left(\frac{t}{T_s}\right) k = 1, 2, \ldots, K \tag{5}$$

where T_s is the symbol interval, $f_k = \frac{k}{T_s}$ is the kth subcarrier, and K is the total number of subcarriers. The relationship between symbol waveforms $s_i(t)$ and constellation points $\mathbf{s}_i = [s_{1,i}, s_{2,i}, \ldots, s_{2K+1,i}]$ is

$$s_i(t) = \underbrace{s_{1,i}\phi_1(t)}_{\text{Adaptive Bias}} + s_{2,i}\phi_2(t) + \cdots + s_{2K+1,i}\phi_{2K+1}(t). \tag{6}$$

At the receiver, a constellation point $\mathbf{s}_i$ is recovered though a set of matched filters. To minimize the system error rate, one way is to maximize the MED between pairs of columns of the following constellation matrix

$$\mathcal{S} = \begin{bmatrix} s_{1,1} & s_{1,2} & \cdots & s_{1,N_c} \\ s_{2,1} & s_{2,2} & \cdots & s_{2,N_c} \\ \vdots & \vdots & \ddots & \vdots \\ s_{2K+1,1} & s_{2K+1,2} & \cdots & s_{2K+1,N_c} \end{bmatrix}$$

subject to illumination constraints. We typically stack the columns into a single vector instead, i.e.

$$\mathbf{s}_J = [\mathbf{s}_1^T\, \mathbf{s}_2^T \ldots \mathbf{s}_{N_c}^T]^T \tag{7}$$

for simplicity of the formulation of the optimization problem discussed in Section II.

III. DC-informative Joint Color-Frequency Modulation with RGB LEDs

Based on the idea discussed in Section II, we propose two constellation design methods taking advantage of the informative dc-bias for a VLC system employing one RGB LED as shown by Fig. 1. If the inputs into R/G/B carry independent bit information as shown by Fig. 1(a), it is termed a decoupled scheme. In comparison, if the inputs into R/G/B modulators carry information jointly, it is a joint scheme instead as shown by Fig. 1(b). In other words, although for a joint scheme still three modulators are used to create continuous domain waveforms to drive corresponding LEDs, information cannot be estimated through recovery of a single (or any pair) of them.

It is observed that the joint scheme may utilize four types of diversities during per channel use, including frequency diversity, color(wavelength) diversity, adaptive dc, and spatial diversity. Spatial diversity can be achieved by extending from employing only one RGB LED to include N ones, which is out of scope of this paper. We only focus on the first three diversities here. This scheme is termed dc-informative joint color-frequency modulation (DCI-JCFM).

The decoupled system shown in Fig. 1(a) works as follows: At the transmitter-side, three independent bit streams $\mathbf{b}_{x,i}, x \in$ [red, green, blue] $i \in [1, N_c]$, of length N_x are mapped to corresponding constellation points $\mathbf{s}_{x,i}$ of size $(2K+1) \times 1$ first, which are modulated separately to generate continuous symbol

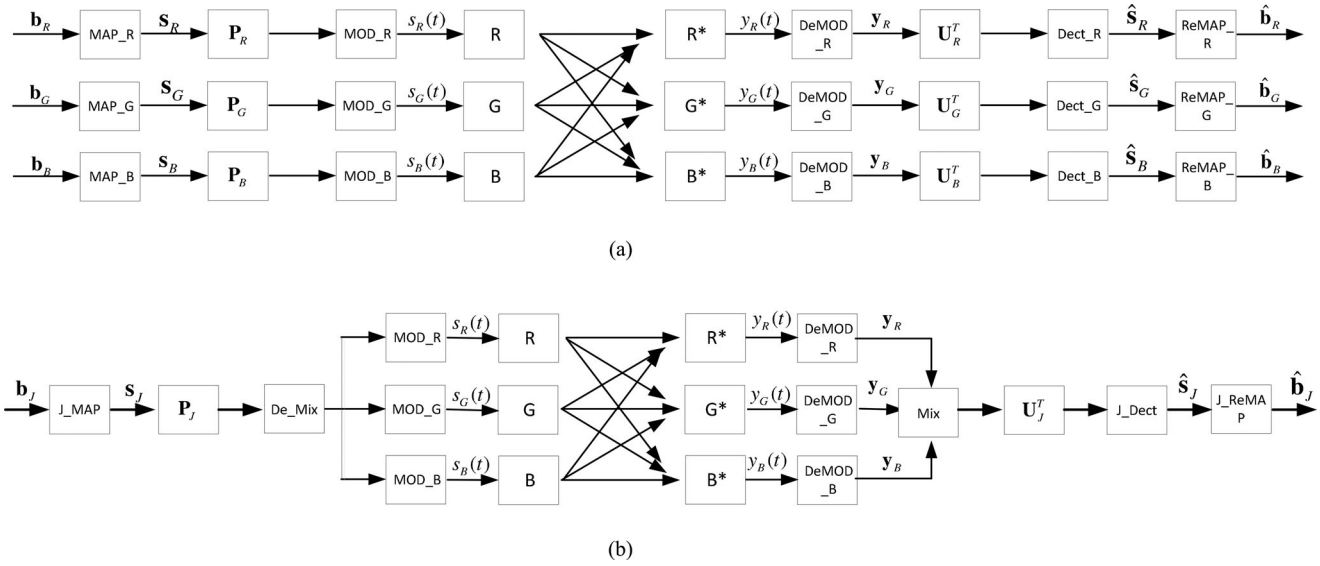

Fig. 1. (a) System block diagram of a decoupled system. (b) System block diagram of the DCI-JCFM. $\big($(Re)MAP$_{\text{R/G/B}}$: bits and constellation (Re)mapper for R/G/B channel; (De)MOD$_{\text{R/G/B}}$: (De)modulator for R/G/B channel; R/G/B*: photo-detector and color filter for R/G/B channel; J$_{\text{(Re)MAP}}$: joint (Re)mapper; J_{Dect}: joint symbol detector$\big)$.

waveform (current) $s_{x,i}(t)$ by (6) for each channel. If cross-talks exist for any channel, a corresponding precoder $\mathbf{P}_x$ needs to be applied before modulation. Waveforms $s_{x,i}(t)$ are then electrical-to-optical converted to intensity signals $\eta s_{x,i}(t)$ to drive the LEDs. At the receiver-side, photo detectors of each channel collect the waveforms (convoluted with channel and corrupted by noise). The received signal is sent through red, green, and blue color filters respectively and after optical-to-electrical conversion waveforms $y_{x,i}(t)$ are obtained. Then, $2K+1$ matched filters are employed for each channel to demodulate $y_{x,i}(t)$ to obtain signal vector $\mathbf{y}_{x,i}$. Three symbol detectors follow to provide $\hat{\mathbf{s}}_{x,i}$, estimates of the symbol vectors, which are de-mapped separately and the estimates of original bit sequences $\mathbf{b}_{x,i}$ are finally obtained. If cross-talks exist, post-equalizers $\mathbf{U}_x^T$ are applied before the symbol detectors.

System using DCI-JCFM as shown by Fig. 1(b) works differently. First, a joint bit sequence

$$\mathbf{b}_J = [\mathbf{b}_{R,i}^T \mathbf{b}_{G,i}^T \mathbf{b}_{B,i}^T]^T \tag{8}$$

is mapped to a higher dimensional constellation point $\mathbf{s}_J$ of dimension $6K+3$, containing coefficients for the RGB color channels. Then, three groups of coefficient sets with dimension $2K+1$ are obtained through a de-mixer, to modulate three color channels, respectively, resulting in, for example, the green signal $s_G(t)$ as follows:

$$s_G(t) = \underbrace{\mathbf{s}_J[2K+2]\phi_1(t)}_{\text{Adaptive Bias}} + \sum_{k=1}^{K}(\mathbf{s}_J[2K+1+2k]\phi_{2k}(t) + \mathbf{s}_J[2K+2+2k]\phi_{2k+1}(t)) \tag{9}$$

and signals for red and blue channels can be written similarly with different sets of coefficients. Note that the 1st, $(2K+2)$th, $(4K+3)$th components in $\mathbf{s}_J$ correspond to the dc-bias for RGB channels, respectively.

If cross-talks exist, a joint precoder $\mathbf{P}_J$ is applied before modulation. Also, we observe the expectation of $s_{J,i}(t)$ as follows:

$$\mathbb{E}[s_{J,i}(t)] = \sum_{p=1}^{3} s_{(p-1)(2K+1)+1,i}\phi_1(t) \tag{10}$$

since all non-dc basis has zero time averages. Therefore, both the average optical power and average color of system are determined solely by these three adaptive dc-bias. While the dynamic range of waveform, instead, is influenced by all subcarriers of all LEDs.

For our design, we will demonstrate with a line-of-sight (LOS) scenario when channel has cross-talks, due to the imperfectness of receiver color filters. The discrete channel model can be written as follows [13]

$$\begin{aligned}\mathbf{y} &= \mathbf{H}\mathbf{s} + \mathbf{n} \\ &= \begin{bmatrix}\mathbf{y}_R \\ \mathbf{y}_G \\ \mathbf{y}_B\end{bmatrix} = \begin{bmatrix}\mathbf{I} & \mathbf{O} & \mathbf{O} \\ \mathbf{O} & (1-2\epsilon)\mathbf{I} & \epsilon\mathbf{I} \\ \mathbf{O} & \epsilon\mathbf{I} & (1-2\epsilon)\mathbf{I}\end{bmatrix}\begin{bmatrix}\mathbf{s}_R \\ \mathbf{s}_G \\ \mathbf{s}_B\end{bmatrix} + \begin{bmatrix}\mathbf{n}_R \\ \mathbf{n}_G \\ \mathbf{n}_B\end{bmatrix}\end{aligned} \tag{11}$$

where $\epsilon \in [0, 0.5]$ is termed the "cross-talk index (CI)" and $\mathbf{n} \sim \mathcal{N}(\mathbf{0}, \mathbf{I} \cdot N_0/2)$.

A. The Objective Function

With working SNRs for VLC, which are typically medium-to-high, the minimum Euclidean distance between constellation pairs governs SER. Therefore, we seek to minimize the system SER by maximizing the minimum Euclidean distance, through carefully design the constellation vector $\mathbf{s}_J$ subject to key lighting constraints. For a system employing a constellation of size N_c, a total of $N_c(N_c-1)/2$ Euclidean distance constraints between symbol $\mathbf{s}_i$ and $\mathbf{s}_j$, where $i, j \in [1, N_c] i \neq j$, are included.

These distance constraints are defined as follows[21]:

$$\mathbf{s}_J^T \mathbf{F}_l \mathbf{s}_J \geq d_{\min}^2, \qquad l = 1 \ldots N_c(N_c-1)/2 \tag{12}$$

where $\mathbf{F}_l$ is a square matrix for calculation of the distance between the lth constellation pair. To illustrate the structure of $\mathbf{F}_l$, we define the integer l as a function of integers p and q, and define

$$\mathbf{F}_{l(p,q)} = \mathbf{E}_{pq} \tag{13}$$

and

$$\mathbf{E}_{pq} = (\mathbf{E}_p - \mathbf{E}_q)^T (\mathbf{E}_p - \mathbf{E}_q) \tag{14}$$

where $\mathbf{E}_p = \mathbf{e}_p^T \otimes \mathbf{I}_{N_c}$ is a matrix composed of zeros and ones, $\otimes$ denotes Kronecker product, $\mathbf{e}_p$ is the pth column of identity matrix $\mathbf{I}_{6K+3}$, and $l(p,q) \cong (p-1)N_c - \frac{p(p+1)}{2} + q, p, q \in 1, 2, \ldots, N_c, p < q$.

The distance constraints are nonconvex in $\mathbf{s}_J$. We choose to use the following linear approximation at point $\mathbf{s}_J^{(0)}$:

$$\mathbf{s}_J^T \mathbf{F}_l \mathbf{s}_J \cong 2\mathbf{s}_J^{(0)T} \mathbf{F}_l \mathbf{s}_J - \mathbf{s}_J^{(0)T} \mathbf{F}_l \mathbf{s}_J^{(0)} \geq d_{\min}^2 \qquad \forall l. \tag{15}$$

B. Practical Lighting Requirements

For our design problem, practical lighting issues considered include average optical power, color of illumination, which is determined by the relative intensity ratios of the RGB components, luminous efficacy rate (LER), which is a measure of how well a light source produces visible light, color rending index (CRI), which is a measure of how well light source reveals the colors of objects faithfully in comparison with an ideal light source, non-negative intensity, and flickering-free requirements. It is worth noting that the CRI constraint is only active for a "balanced system," i.e., white-light illumination is required, thus the first three requirements can be constraint using only one equation written as follows:

$$P_o \cdot \mathbf{s}_{\text{avg}} = \frac{1}{N_c} \mathbf{J} \mathbf{s}_J \tag{16}$$

where P_o is the average optical power of a RGB LED, $\mathbf{J}$ is a $3 \times (6K+3)N_c$ selection matrix (containing only ones and zeros) adding up R/G/B components in $\mathbf{s}_J$, respectively, by a multiplication of each row with it, $\mathbf{s}_{\text{avg}} = [s_R s_G s_B]^T$ is termed the average color ratio vector and the following equation holds

$$s_R + s_G + s_B = 1. \tag{17}$$

In this paper, we assume $\mathbf{s}_{\text{avg},B} = [1/3, 1/3, 1/3]^T$ for a balanced system, $\mathbf{s}_{\text{avg},U} = [4/9, 3/9, 2/9]^T$ for an unbalanced system, $\mathbf{s}_{\text{avg},VU} = [0.7, 0.15, 0.15]^T$ and for a very unbalanced system.

Thus, the optical power and illumination color requirements are constrained together. The luminous efficacy rate and color rendering index requirements can be satisfied by properly choosing $\mathbf{s}_{\text{avg}}$.

C. Dynamic Range Requirement

Since the linear dynamic range of LEDs is limited, the ranges of signal for each LED have to be constrained to avoid nonlinear distortion, i.e.

$$0 \leq s_{x,i}(t) \leq I_U \qquad \forall x, i \tag{18}$$

where I_U is the highest current level, and for simplicity, we have assumed that RGB LEDs have the same dynamic range. We propose to constrain dynamic range of a sequence of sampled signal

$$0 \leq s_{x,i}(t_n) \leq I_U \qquad \forall x, i \tag{19}$$

and t_n is picked as

$$t_n = \frac{nT_s}{2KN_o}, \qquad n = 0, 1, \ldots, N \tag{20}$$

where N_o is the oversampling rate, $N = 2KN_o$, and $N+1$ is the total number of sample points. It should be noted that although (19) does not guarantee (18), which means the continuous signal waveforms designed subject to (19) could result in negative amplitudes in between the sample instances, the negative peak is very small compare to the dynamic range of signal. We can compensate this effect by adding a small post dc-bias after obtaining an optimized constellation.

Therefore, we can formulate this point-wise dynamic range constraints as follows:

$$\mathbf{u}_n^T \mathbf{K}_x \mathbf{J}_i \mathbf{s}_J \geq 0, \qquad \forall (x, i, n) \tag{21}$$

$$\mathbf{u}_n^T \mathbf{K}_x \mathbf{J}_i \mathbf{s}_J \leq I_U, \qquad \forall (x, i, n) \tag{22}$$

where $\mathbf{J}_i$ selects the ith constellation point and $\mathbf{K}_x$ selects the corresponding coefficients for color x, $\mathbf{u}_n = [u_{n,0}, u_{n,1}^c, u_{n,1}^s, \ldots, u_{n,K}^c, u_{n,K}^s]^T$, $u_{n,0} = \sqrt{1/T_s}$, $u_{n,k}^c = \sqrt{2/T_s}\cos(2\pi f_k t_n)$, and $u_{n,k}^s = \sqrt{2/T_s}\sin(2\pi f_k t_n)$.

D. Problem Formulation

We first formulate the optimization problem when there are no cross-talks among different colored LEDs, i.e., $\mathbf{H} = \mathbf{I}$, as follows:

$$\begin{aligned} \underset{\mathbf{s}_J, d_{\min,J}}{\text{maximize}} \quad & d_{\min,J} \\ \text{s.t.} \quad & P_o \cdot \mathbf{s}_{\text{avg}} = \frac{1}{N_c} \mathbf{J} \mathbf{s}_J \\ & 2\mathbf{s}_J^{(0)T} \mathbf{F}_l \mathbf{s}_J - \mathbf{s}_J^{(0)T} \mathbf{F}_l \mathbf{s}_J^{(0)} \geq d_{\min,J}^2 \qquad \forall l. \\ & \mathbf{u}_n^T \mathbf{K}_x \mathbf{J}_i \mathbf{s}_J \geq 0 \qquad \forall (x, i, n) \\ & \mathbf{u}_n^T \mathbf{K}_x \mathbf{J}_i \mathbf{s}_J \leq I_U \qquad \forall (x, i, n) \end{aligned} \tag{23}$$

which is convex, due to the fact that both the objective function and constraints are jointly convex with respect to the optimization parameters $d_{\min,J}$ and $\mathbf{s}_J$. Thus, specialized solver such as CVX toolbox for MATLAB can be utilized [22]. Starting from initial point $\mathbf{s}_J^{(0)}$, the scheme can iteratively converge to a local optima with each run. The best constellation is chosen from local optimal constellation obtained from multiple runs.

When the channel suffers from cross-talks, we choose to deal with it by employing the well-known singular value decomposition (SVD) based pre-equalizer $\mathbf{P} = \mathbf{V}\mathbf{S}^{-1}$ and post-equalizer

$\mathbf{U}^H$ for our system, where $\mathbf{H} = \mathbf{USV}^H$. Constellation is designed by an optimization with transformed constraints as follows:

$$\begin{aligned} \underset{\mathbf{s}_J, d_{\min,J}}{\text{maximize}} \quad & d_{\min,J} \\ \text{s.t.} \quad & P_o \cdot \mathbf{s}_{\text{avg}} = \frac{1}{N_c}\mathbf{J}\mathbf{P}_J\mathbf{s}_J \\ & 2\mathbf{s}_J^{(0)T}\mathbf{F}_l\mathbf{s}_J - \mathbf{s}_J^{(0)T}\mathbf{F}_l\mathbf{s}_J^{(0)} \geq d_{\min,J}^2 \qquad \forall l. \\ & \mathbf{u}_n^T\mathbf{K}_x\mathbf{J}_i\mathbf{P}_J\mathbf{s}_J \geq 0 \qquad \forall(x,i,n) \\ & \mathbf{u}_n^T\mathbf{K}_x\mathbf{J}_i\mathbf{P}_J\mathbf{s}_J \leq I_U \qquad \forall(x,i,n) \end{aligned} \tag{24}$$

where $\mathbf{P}_J = \mathbf{I}_{N_c} \otimes \mathbf{P}$ is defined. This problem is convex, since multiplication of $\mathbf{s}_J$ with a fixed matrix $\mathbf{P}_J$ does not affect the joint convexity of the objective function and constraints with respect to the optimization parameters $d_{\min,J}$ and $\mathbf{s}_J$.

For the decoupled system, three independent problems can be formulated to find the MEDs for color $x = [\text{Red, Green, Blue}]$, i.e.

$$\begin{aligned} \underset{\mathbf{s}_x, d_{\min,x}}{\text{maximize}} \quad & d_{\min,x} \\ \text{s.t.} \quad & P_o \cdot s_x = \frac{1}{N_c}\mathbf{j}^T\mathbf{P}_x\mathbf{s}_x \\ & 2\mathbf{s}_x^{(0)T}\tilde{\mathbf{F}}_l\mathbf{s}_x - \mathbf{s}_x^{(0)T}\tilde{\mathbf{F}}_l\mathbf{s}_x^{(0)} \geq d_{\min,x}^2 \qquad \forall l. \\ & \mathbf{u}_n^T\tilde{\mathbf{J}}_i\mathbf{P}_x\mathbf{s}_x \geq 0 \qquad \forall(i,n) \\ & \mathbf{u}_n^T\tilde{\mathbf{J}}_i\mathbf{P}_x\mathbf{s}_x \leq I_{u,x} \forall(i,n) \end{aligned} \tag{25}$$

where $d_{\min,x}$, $\mathbf{j}$, $\mathbf{P}_x$, $\tilde{\mathbf{F}}_l$, $\tilde{\mathbf{J}}_i$, and $I_{U,x}$ are defined in a similar manner with corresponding parameters in (24). For brevity, we omit the explicit definitions.

IV. Dynamic Range Versus PAPR Constraints

Although a constraint on the dynamic range of symbol waveforms can eliminate non-linear distortion, it may result in a non-affordable decrease in power-efficiency, especially when only few symbol waveforms among all suffer from larger dynamic range.

Alternatively, one can consider using certain PAPR constraint instead of the dynamic range constraint. Since RGB LEDs are employed, it is necessary that the PAPRs of $s_R(t)$, $s_G(t)$, and $s_B(t)$ are constrained individually. There are in general two types of PAPR constraints, the so-called long-term PAPR (L-PAPR) and short-term PAPR (S-PAPR).

The L-PAPR is defined as the peak of all symbol waveforms over the average power in a long run. With an L-PAPR constraint, the PAPR of certain sub waveform can be notably larger/smaller than the rest. Mathematically, with the L-PAPR constraint the color $x \in [R, G, B]$ LED is written as follows:

$$\begin{aligned} \Phi_x(\mathbf{s}_J) &= \frac{[\max_{i,n}(\mathbf{u}_n^T\mathbf{K}_x\mathbf{J}_i\mathbf{s}_J)]^2}{\mathbf{s}_J^T\mathbf{s}_J/N_c} \\ &= \frac{N_c[\max_{i,n}(\mathbf{u}_n^T\mathbf{K}_x\mathbf{J}_i\mathbf{s}_J)]^2}{\mathbf{s}_J^T\mathbf{s}_J} \leq \beta_x \end{aligned} \tag{26}$$

where $\max_{i,n}(\mathbf{u}_n^T\mathbf{K}_x\mathbf{J}_i\mathbf{s}_J)$ denotes the peak amplitude of all symbol waveforms, $\mathbf{s}_J^T\mathbf{s}_J/N_c$ denotes the average power, β_x is the maximally allowable PAPR for the color x LED. These constraints are transformed into the following form:

$$\mathbf{u}_n^T\mathbf{K}_x\mathbf{J}_i\mathbf{s}_J - \sqrt{\frac{\beta_x\mathbf{s}_J^T\mathbf{s}_J}{N_c}} \leq 0 \qquad \forall(i,n) \tag{27}$$

which is non-convex in $\mathbf{s}_J$, due to the second term in (27), thus is transformed into a convex one by approximating (27) at the initial point $\mathbf{s}_J^{(0)}$ as picked in (15) as follows:

$$\mathbf{u}_n^T\mathbf{K}_x\mathbf{J}_i\mathbf{s}_J - \sqrt{\frac{\beta_x}{N_c}}(\mathbf{s}_J^{(0)T}\mathbf{s}_J^{(0)})^{-\frac{1}{2}}\mathbf{s}_J^{(0)T}(\mathbf{s}_J - \mathbf{s}_J^{(0)}) \leq 0 \forall(i,n) \tag{28}$$

where a linear (thus, convex) constraint is obtained.

When the probabilities of occurrence of different sub waveforms are unequal, it might be wiser to consider the short-term PAPRs (S-PAPRs) instead, which is defined as the ratios of the peak power of each waveform over its average power. Among N_c waveforms, the S-PAPR for the ith waveform and the color x LED is defined as follows:

$$\Phi_{x,i}(\mathbf{s}_J) = \frac{[\max_n(\mathbf{u}_n^T\mathbf{K}_x\mathbf{J}_i\mathbf{s}_J)]^2}{\mathbf{s}_J^T\mathbf{J}_i^T\mathbf{J}_i\mathbf{s}_J} \leq \beta_{x,i} \tag{29}$$

where $\max_n(\mathbf{u}_n^T\mathbf{K}_x\mathbf{J}_i\mathbf{s}_J)$ denotes the peak amplitude value of the ith sub waveform, $\mathbf{s}_J^T\mathbf{J}_i^T\mathbf{J}_i\mathbf{s}_J$ denotes its power, and $\beta_{x,i}$ is the maximally allowable S-PAPR. These constraints are transformed into the following form:

$$\mathbf{u}_n^T\mathbf{K}_x\mathbf{J}_i\mathbf{s}_J - \sqrt{\beta_{x,i}\mathbf{s}_J^T\mathbf{J}_i^T\mathbf{J}_i\mathbf{s}_J} \leq 0 \qquad \forall n \tag{30}$$

and a similar linear approximation process is applied to convert them into convex constraints.

An interesting observation recently in [24] shows that the non-linearity mitigation for an IM/DD VLC is a more involved problem than expected. The reason is that the lower baseband frequency parts are causing larger non-linear distortion than the higher frequency parts. This effect, if taken into account along with the three constraints discussed previously, is expected to make the design problem even more worthwhile to look into.

V. Performance Evaluation

In this section, we compare the performances of the decoupled scheme and DCI-JCFM by assessing the maximum MED and bit error rate (BER) under different channel cross-talk and color illumination assumptions.[3] Each constellation point is assumed to have equal probability of transmission, and the union bound for SER of both schemes can be written as [10, Eq. (25)]

$$P_{e,s} \approx \frac{2N_n}{N_c}Q\left(\sqrt{\frac{d_{\min,z}^2}{2N_0}}\right) \tag{31}$$

where N_n is the number of neighbor constellation pairs [10] and

$$Q(x) = \frac{1}{\sqrt{2\pi}}\int_x^\infty \exp(-t^2/2)dt \tag{32}$$

[3]A binary switching algorithm (BSA) is applied to optimally map bit sequences to constellation points [23].

TABLE I
MED COMPARISON WITH NO CROSS-TALK, DCI-JCFM (ROW 1&2) VERSUS DECOUPLED (ROW 3&4)

$d_{\min,z}$	Balanced	Unbalanced	Very Unbalanced
$K=2$	19.995	19.588	18.020
$K=3$	24.818	24.559	22.752
$K=2$	[13.18,13.18,13.18]	[15.90,11.93,7.95]	[27.68,5.93,5.93]
$K=3$	[15.03,15.03,15.03]	[18.04,13.53,9.02]	[31.56,6.76,6.76]

denotes the Gaussian Q-function, $d_{\min,z\in[J,R,G,B]}$ stands for the MED of the DCI-JCFM and MEDs for decoupled schemes. The BER is thus calculated as

$$P_{e,b} = \frac{\lambda}{N_b} P_{e,s} \tag{33}$$

where λ is the number of wrongly detected bits in each bit sequence, which can be minimized by employing the BSA mapper.

A. System Comparison With No Channel Cross-Talk

We first compare the DCI-JCFM and the decoupled scheme when channel cross-talks do not exist. To guarantee a fair comparison, the following system parameters are chosen: the number of Monte-Carlo runs for each scheme $N_M = 20$, the length of bit sequence for each channel use is $N_b = 6$ for DCI-JCFM and $N_{b_{R/G/B}} = 2$, respectively, for each channel of the decoupled system, the number of subcarriers for each LED is $K = 2$ or 3, the average optical power $P_o = 20$, the symbol interval $T_s = 1$ is used without loss of generality since the design is rate independent. The MEDs of the two schemes for three systems obtained through picking the best constellation from the 20 local optimums are summarized by Table I.

From Table I, key observations include: 1) With the DCI-JCFM, the "joint MED" is much larger than the R/G/B "decoupled MEDs," except for the cases with very unbalanced illumination. While for the very unbalanced case, the blue and green channels could suffer from severe performance loss with the small MEDs, and therefore, the DCI-JCFM is still expected to work better. 2) Larger MEDs are obtained with an increased number of subcarriers. We are only listing the cases when $K = 2$ and $K = 3$ for brevity, while we have observed through additional simulations that this gain continue to grow with K. 3) The more balanced a system is, the better performance is expected.

B. DCI-JCFM Performance With Channel Cross-Talk

With $K = 2$ and other parameters given the same values as in the previous section for DCI-JCFM, we simulate to obtain the best MEDs subject to different cross-talk levels, controlled by CI varying from [0,0.2] (since with only average quality color filters CI beyond 0.2 can be avoided).

From Table II, key observations include: 1) with increased channel cross-talks, the performances of all system degrade monotonously; 2) the performance of the balanced system remains the best with any level of channel cross-talks; and 3) the DCI-JCFM shows robustness to cross-talks, since with a severe cross-talk level, i.e., $\epsilon = 0.2$, the system performance does not suffer from a significant MED drop.

TABLE II
MED WITH DIFFERENT CROSS-TALK LEVELS, DCI-JCFM

$d_{min,z}$	Balanced	Unbalanced	Very Unbalanced
$\epsilon = 0$	19.995	19.588	18.020
$\epsilon = 0.05$	18.834	18.798	17.014
$\epsilon = 0.1$	16.898	16.835	16.346
$\epsilon = 0.15$	15.334	15.037	15.192
$\epsilon = 0.2$	14.444	14.250	14.273

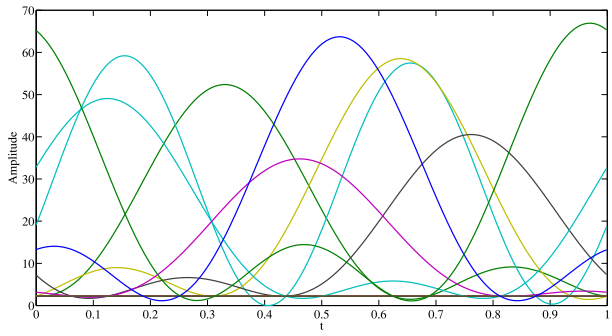

Fig. 2. Set of sub waveforms for DCI-JCFM red channel with $K = 2$, $I_U = 70$.

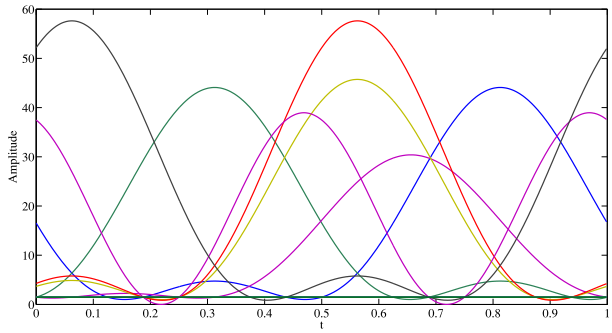

Fig. 3. Set of sub waveforms for DCI-JCFM green channel with $K = 2$, $I_U = 70$.

C. The Designed Symbol Waveforms With DCI-JCFM

We pick the optimized constellation $\mathbf{s}_J^*$ designed for unbalanced system as an example in this section. If cross-talks do not exist, the sets of subcarrier symbol waveforms $s_{R,i}(t), s_{G,i}(t), s_{B,i}(t) \forall i$ obtained with DCI-JCFM are plotted in Figs. 2–4. With each figure, the symbol waveforms are differentiated by color. The parameters associated are: average optical power $P_0 = 20$, number of bits per symbol $N_b = 4$, number of subcarriers $K = 2$, peak amplitude $I_U = 70$, no cross-talks and varying noise power. It is possible that $s_{x,i*}(t) = s_{x,j*}(t)$ with some $i \neq j$ for the color x LED, as long as $s_{y,i*} \neq s_{y,j*}$ for the LED with color $y \in [R, G, B], y \neq x$. Therefore, the number of sub waveforms is less or equal to 2^{N_b}. Fig. 5 presents bit error rate curves of the two schemes under "Balanced," "Unbalanced," and "Very Unbalanced" illumination with varying optical signal to noise ratio. Note that since the average optical power $P_o = 20$ is fixed in the simulations, it is most reasonable to evaluate the system performance with respect to selected

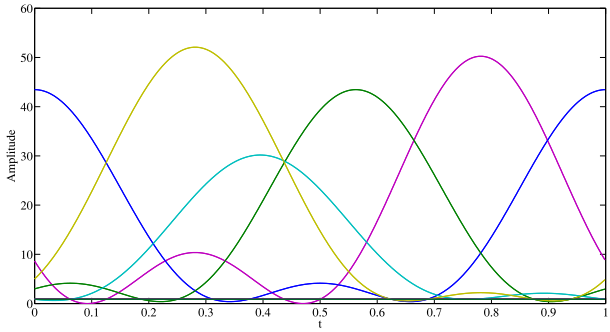

Fig. 4. Set of sub waveforms for DCI-JCFM blue channel with $K = 2$, $I_U = 70$.

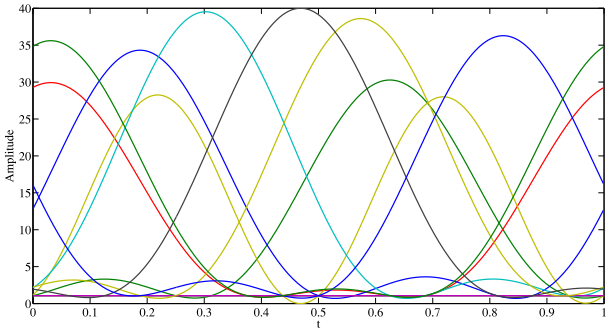

Fig. 7. Set of sub waveforms for DCI-JCFM green channel with $K = 2$, $I_U = 40$.

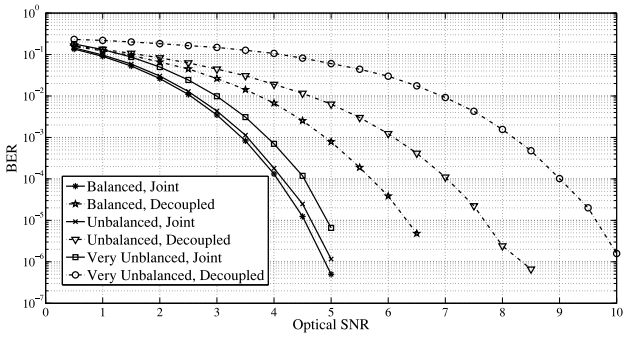

Fig. 5. BER performance of DCI-JDCM and the decouple scheme, $N_b = 6$, $K = 2$, $I_U = 70$, no cross-talks.

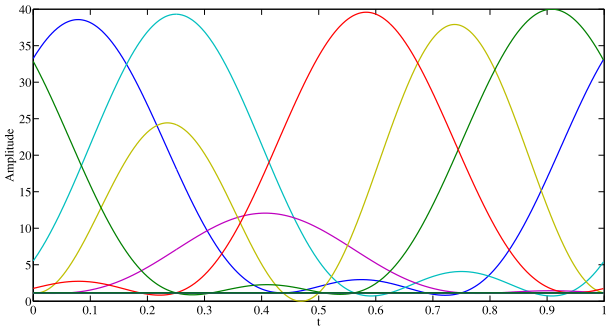

Fig. 8. Set of sub waveforms for DCI-JCFM blue channel with $K = 2$, $I_U = 40$.

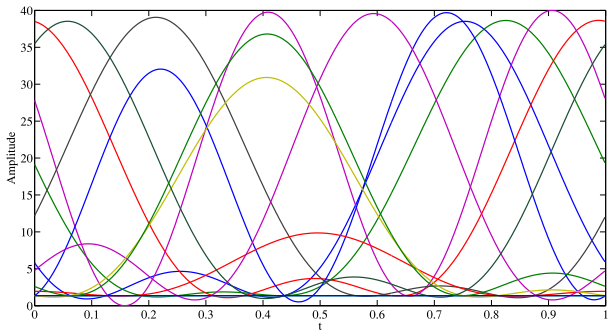

Fig. 6. Set of sub waveforms for DCI-JCFM red channel with $K = 2$, $I_U = 40$.

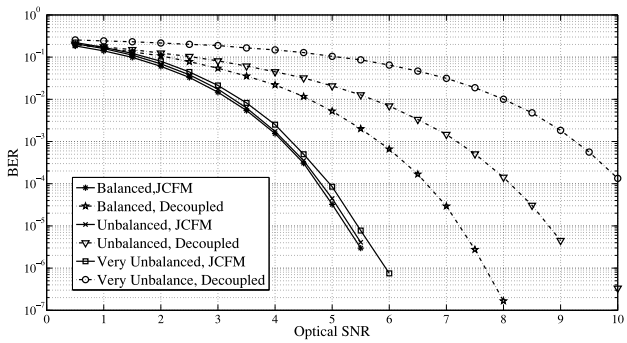

Fig. 9. BER performance of DCI-JDCM and the decouple scheme, $N_b = 6$, $K = 2$, $I_U = 70$, $\epsilon = 0.1$.

working optical SNRs. Of course, comparison under fixed average electrical power P_e can be made in a similar manner as well, with properly define the electrical SNR instead. The optical SNR is defined as [10, Eq. (27)]

$$\gamma_o = 10 \log_{10} \frac{P_o}{\sqrt{N_b N_0}} \tag{34}$$

assuming the electrical-to-optical conversion factor $\alpha = 1$. Significant power gains of the DCI-JCFM over the decoupled scheme are observed. Also, more unbalanced system suffers from worse performance. If the peak amplitude $I_U = 40$, the corresponding subcarrier symbol waveforms are plotted in Figs. 6–8. By simulations, it is observed that the MED drops from 27.70 to 25.67 when the peak amplitude changes from 70 to 40, where the latter corresponds to a 3dB L-PAPR. In Fig. 9, with assuming non-zero cross-talk, where $\epsilon = 0.1$, the BER performance comparison between the two schemes is presented.

VI. Conclusion

We have proposed a joint constellation design scheme termed DCI-JCFM taking advantage of the wavelength, frequency, and adaptive bias diversities at the same time for indoor VLC systems. By applying the DCI-JCFM scheme, waveform symbols with a much larger MED can be obtained than those from a decoupled scheme with or without channel cross-talks. In the future, we will make a comprehensive power-efficiency comparison between the proposed DCI-JCFM scheme and the

conventional MSM scheme under the same spectral efficiency. We will also develop complexity-reduced algorithms for cases where the visible light channel changes fast. Moreover, we will design advanced precoders to replace the SVD-based pre and post-equalizers utilized in this paper.

REFERENCES

[1] T. Komine and M. Nakagawa, "Fundamental analysis for visible light communication system using LED lights," *IEEE Trans. Consum. Electron.*, vol. 50, no. 1, pp. 100–107, Feb. 2004.

[2] S. Rajagopal, R. Roberts, and S. Lim, "IEEE 802.15.7 visible light communication: Modulation schemes and dimming support," *Opt. Exp.*, vol. 16, no. 26, pp. 21835–21842, Dec. 2008.

[3] H. Elgala, R. Mesleh, and H. Haas, "Indoor optical wireless communication: Potential and state-of-the-art," *IEEE Commun. Mag.*, vol. 49, no. 9, pp. 56–63, Sep. 2011.

[4] L. Zeng, D. O'Brien, H. Minh, G. Faulkner, K. Lee, D. Jung, Y. Oh, and E. Won, "High data rate multiple input multiple output (MIMO) optical wireless communications using white LED lighting," *J. Sel. Area Commun.*, vol. 27, no. 9, pp. 1654–1662, 2009.

[5] J. Armstrong, "OFDM for optical communications," *J. Lightw. Technol.*, vol. 27, no. 3, pp. 189–204, Feb. 2009.

[6] S. Dimitrov, S. Sinanovic, and H. Haas, "Clipping noise in OFDM-Based optical wireless communication systems," *IEEE Trans Commun.*, vol. 60, no. 4, pp. 1072–1081, Apr. 2012.

[7] D. Bykhovsky and S. Shlomi, "An experimental comparison of different bit-and-power-allocation algorithms for DCO-OFDM," *J. Lightw. Technol.*, vol. 60, no. 4, pp. 1559–1564, Apr. 2014.

[8] R. You and J. Kahn, "Average power reduction techniques for multiple-subcarriers intensity-modulated optical signals," *IEEE Trans. Commun.*, vol. 49, no. 12, pp. 2164–2170, Dec. 2001.

[9] S. Teramoto and T. Ohtsuki, "Multiple-subcarrier optical communication systems with subcarrier signal-point sequence," *IEEE Trans. Commun.*, vol. 53, no. 10, pp. 1738–1743, Oct. 2005.

[10] J. Karout, E. Agrell, K. Szczerba, and M. Karlsson, "Optimizing constellations for single-subcarrier intensity modulated optical systems," *IEEE Trans. Inf. Theory*, vol. 58, no. 7, pp. 4645–4659, Jul. 2012.

[11] Q. Gao, J. H. Manton, G. Chen, and Y. Hua, "Constellation design for a multicarrier optical wireless communication channel," *IEEE Trans. Commun.*, vol. 62, no. 1, pp. 214–225, Jan. 2014.

[12] Q. Gao, L. Liao, G. Chen, and Y. Hua, "Free-space optical multi-subcarrier communication employing power-efficient constellations." in *Proc. IEEE 15th Int. Workshop Signal Process. Advances Wireless Commun.*, 2014, pp. 379–383.

[13] E. Monteiro and S. Hranilovic, "Constellation design for color-shift keying using interior point methods," *IEEE Opt. Wireless Commun. Workshop*, Dec. 2012, pp. 1224–1228.

[14] G. Cossu, A. M. Khalid, P. Choudhury, and E. Ciaramella, "3.4 Gbit/s visible optical wireless transmission based on RGB LED," *Opt. Exp.*, vol. 20, no. 26, pp. B501–B506, 2012.

[15] B. Bai, Q. He, Z. Xu, and Y. Fan, "The color shift key modulation with non-uniform signaling for visible light communication," in *Proc. 1st Int. Workshop Opt. Wireless Commun. China*, 2012, pp. 37–42.

[16] J. Vucic, C. Kottke, K. Habel, and K. D. Langer, "803 Mbit/s Visible Light WDM Link based on DMT Modulation of a Single RGB LED Luminary," presented at the *Optical Fiber Communication Conf.*, Los Angeles, CA, USA, Mar. 2011.

[17] IEEE 802.15.7 Visible Light Communication Task Group. (2010, Aug. 30). IEEE 802.15 Documents [Online]. Available: https://mentor.ieee.org/802.15/documents?is group=0007.

[18] CIE, "Colour rendering (TC 1-33 closing remarks)," Publication 135/2, CIE Central Bureau, Vienna, Austria, 1999.

[19] A. Stimson, "*Photometry and Radiometry for Engineers,*" New York, NY, USA: Wiley, 1974.

[20] S. Han and J. Lee, "An overview of peak-to-average power ratio reduction techniques for multicarrier transmission," *IEEE Trans. Wireless Commun.*, vol. 9, no. 2, pp. 523–527, Apr. 2005.

[21] M. Beko and R. Dinis, "Designing good multi-dimensional constellations," *IEEE Wireless Commun. Lett.*, vol. 1, no. 3, pp. 221–224, Jun. 2012.

[22] CVX Users' Guide, CVX Research, Inc., Austin, TX, USA.

[23] F. Schreckenbach, N. Gortz, J. Hagenauer, and G. Bauch, "Optimization of symbol mappings for bit-interleaved coded modulation with iterative decoding," *IEEE Commun. Lett.*, vol. 7, no. 12, pp. 593–595, Dec. 2003.

[24] J. Li, Z. Huang, X. Liu, and Y. Ji, "Hybrid time-frequency domain equalization for LED nonlinearity mitigation in OFDM-based VLC systems," *Optics Express*, vol. 23, no. 1, pp. 611–619, 2015.

Qian Gao (M'13) received the M.Sc. and Ph.D. degrees from the University of California, Riverside, CA, USA, in 2010 and 2014, respectively.

He is currently on the faculty of the University of Science and Technology of China. Multiple research projects he contributed in were reported by US core medium. His research interests include signal processing in radio frequency, visible light communication and ultraviolet communication networks, statistical and array signal processing, applications of linear algebra and optimization methods, and advanced modulation design for optical systems. He serves as a Reviewer of the IEEE, OSA, and SPIE journals.

Rui Wang (M'14) received the B.S. degree from Anhui Normal University, Wuhu, China, in 2006, and the M.S. degree from Shanghai University, Shanghai, China, in 2009, and the Ph.D. degree from Shanghai Jiao Tong University, in 2013, all in electronic engineering. From August 2012 to February 2013, he was a visiting Ph.D. student at the Department of Electrical Engineering of University of California, Riverside, CA, USA. From October 2013 to October 2014, he was with the Institute of Network Coding, The Chinese University of Hong Kong as a Postdoctoral Research Associate. Since October 2014, he has been with the College of Electronics and Information Engineering, Tongji University, Shanghai, as an Assistant Professor. His research interests include wireless cooperative communications, MIMO technique, network coding, and OFDM etc.

Zhengyuan Xu (SM'02) received the B.S. and M.S. degrees from Tsinghua University, Beijing, China, in 1989 and 1991, respectively, and the Ph.D. degree from the Stevens Institute of Technology, Hoboken, NJ, USA, in 1999. From 1991 to 1996, he was with Tsinghua Unisplendour Group Corporation, Tsinghua University, as a System Engineer and Department Manager. In 1999, he joined the University of California, Riverside, CA, USA, first as an Assistant Professor, and then, a tenured Associate Professor and Professor. He was the Founding Director of the multi-campus Center for Ubiquitous Communication by Light (UC-Light), University of California. In 2010, he was selected by the Thousand Talents Program of China, appointed as a Professor at Tsinghua University, and then, joined University of Science and Technology of China (USTC). He is the Founding Director of the Optical Wireless Communication and Network Center of USTC, Founding Director of Wireless-Optical Communications Key Laboratory of Chinese Academy of Sciences, and a Chief Scientist of the National Key Basic Research Program (973 Program) of China. His research interests include wireless communication and networking, optical wireless communications, geolocation, intelligent transportation, and signal processing. He has published more than 200 journal and conference papers. He has served as an Associate Editor and Guest Editor for different IEEE journals, and serves as an Associate Editor for the OSA/SIOM journal Photonics Research and the Guest Editor for IEEE JSAC—Special Issue on Optical Wireless Communications. He was a Founding Chair of IEEE Workshop on Optical Wireless Communications.

Yingbo Hua (S'86–M'88–SM'92–F'02) received the B.S. degree from Southeast University, Nanjing, China, in 1982 and the Ph.D. degree from Syracuse University, Syracuse, NY, USA, in 1988. He held a faculty position with the University of Melbourne, Australia, where he was promoted to the rank of a Reader and an Associate Professor in 1996. He was a visiting Professor with the Hong Kong University of Science and Technology (1999–2000), and a Consultant with Microsoft Research, Redmond, WA, USA, (summer 2000). Since 2001, he has been a Professor with the University of California, Riverside, CA, USA.

He has served as the Editor, Guest Editor, Member of Editorial Board and/or Member of Steering Committee for theIEEE TRANSACTIONS ON SIGNAL PROCESSING, IEEE SIGNAL PROCESSING LETTERS, *EURASIP Signal Processing*,IEEE SIGNAL PROCESSING MAGAZINE, IEEE JOURNAL OF SELECTED AREAS IN COMMUNICATIONS, and IEEE WIRELESS COMMUNICATION LETTERS. He has been a Member of the IEEE Signal Processing Society's Technical Committees for Underwater Acoustic Signal Processing, Sensor Array and Multichannel Signal Processing, and Signal Processing for Communication and Networking. He has served on Technical and/or Organizing Committees for more than 50 international conferences and workshops. He has authored/coauthored more than 300 articles and coedited three volumes of books, with more than 8000 citations, in the fields of Sensing, Signal Processing, and Communications. He is a Fellow of the AAAS.